Characterization of Some New Olefinic Block Copolymers

H. P. Wang,† D. U. Khariwala,† W. Cheung,‡ S. P. Chum,‡ A. Hiltner,*,† and E. Baer†

Department of Macromolecular Science, and Center for Applied Polymer Research, Case Western Reserve University, Cleveland, Ohio 44106-7202, and Polyolefins and Elastomers R & D, The Dow Chemical Company, Freeport, Texas 77541

Received July 25, 2006; Revised Manuscript Received January 17, 2007

ABSTRACT: Exciting new developments in polyolefin synthesis give rise to olefinic block copolymers with properties typical of thermoplastic elastomers. The blocky copolymers synthesized by chain shuttling technology consist of crystallizable ethylene−octene blocks with low comonomer content and high melting temperature (hard blocks), alternating with amorphous ethylene−octene blocks with high comonomer content and low glass transition temperature (soft blocks). This paper describes the materials science of these unique polymers as characterized by thermal analysis, X-ray diffraction, microscopy, and tensile deformation. The crystallizable nature of the hard block and the crystalline morphologies are consistent with an average hard block length that is well in excess of 200 carbon atoms. The crystallizable blocks are long enough to form well-organized lamellar crystals with the orthorhombic unit cell and high melting temperature. The lamellae are organized into space-filling spherulites in all compositions even in copolymers with only 18 wt % hard block. The morphology is consistent with crystallization from a miscible melt. Crystallization of the hard blocks forces segregation of the noncrystallizable soft blocks into the interlamellar regions. Good separation of hard and soft blocks in the solid state is confirmed by distinct and separate β- and α-relaxations in all the blocky copolymers. Compared to statistical ethylene−octene copolymers, the blocky architecture imparts a substantially higher crystallization temperature, a higher melting temperature and a better organized crystalline morphology, while maintaining a lower glass transition temperature. The differences between blocky and statistical copolymers become progressively more apparent as the total comonomer content increases.

Introduction

Contemporary advances in catalyst technology allow statistical copolymerization of ethylene with high levels of comonomer.[1] Homogeneous ethylene−octene copolymers with low crystallinity and low density (0.86−0.88 g cm^{-3}) exhibit the characteristics of thermoplastic elastomers.[2] The elastomeric properties depend on the fringed micellar crystals which serve as network junctions.[3,4] However, these elastomers have a low melting temperature which limits their application at higher temperatures.

Commercially important thermoplastic elastomers possess a blocky chain structure consisting of a high melting or high glass transition block and a low melting or low glass transition block.[5] The hard blocks form domains that serve as reinforcements and as physical cross-links to connect the elastomeric soft blocks. The concept of an olefin-based block copolymer would combine high melting, crystallizable hard blocks with amorphous, elastomeric soft blocks.

Early attempts to produce olefinic block copolymers sought to combine crystallizable isotactic[6−9] or syndiotactic[10−12] polypropylene (iPP or sPP) blocks and rubbery amorphous ethylene−propylene copolymers (EPR) using Ziegler−Natta catalysts, but were not commercially successful. Either the products were primarily blends of isotactic PP and amorphous copolymers,[6−9] or the activity of the catalyst was very low.[12] Recently stereoblock polypropylenes have been reported.[13−17] Although the isotactic or syndiotactic polypropylene blocks impart a high melting temperature, the relatively high glass transition temperature of the atactic blocks excludes many elastomeric applications. More recently, olefinic block copolymers containing amorphous blocks with lower T_g, such as iPP-*b*-EPR, sPP-*b*-EPR, and PE-*b*-(ethylene-*co*-hexene) (PE-*b*-PH), have been synthesized using living single-site catalysts.[18,19] The block length and composition can be precisely controlled through sequential monomer addition strategies. However, because it is a batch process and requires a low reaction temperature, this approach is not economically attractive.

Another approach to olefinic block copolymers is hydrogenation of anionically polymerized block copolymers of 1,4-butadiene and isoprene to yield crystallizable polyethylene blocks and amorphous ethylene−propylene copolymer blocks. Diblock,[20−23] triblock,[24−28] and multiblock copolymers[29] have been prepared by this indirect route. Although this is not a practical route to commercial development of olefinic block copolymers, these copolymers provide excellent models for exploring the structure−property relationships.

Exciting new developments in polyolefin synthesis by The Dow Chemical Company enable synthesis of olefinic block copolymers in a direct way.[30] The blocky copolymers synthesized by chain shuttling technology consist of crystallizable ethylene−octene blocks with very low comonomer content and high melting temperature, alternating with amorphous ethylene−octene blocks with high comonomer content and low glass transition temperature. They have a statistical multiblock architecture with a distribution in block lengths and a distribution in the number of blocks per chain. The molecular architecture differs from the well-defined block lengths of olefinic block copolymers synthesized batchwise by anionic polymerization. This paper describes the solid-state structure and properties of the new blocky ethylene−octene copolymers. Comparisons are made with conventional statistical copolymers, as well as with

* Corresponding author. E-mail: ahiltner@case.edu.
† Department of Macromolecular Science, and Center for Applied Polymer Research, Case Western Reserve University.
‡ Polyolefins and Elastomers R & D, The Dow Chemical Company.

10.1021/ma061680e CCC: $37.00
Published on Web 03/14/2007

Table 1. Characteristics of Blocky Ethylene−Octene Copolymers

material	short code	total octene content (wt %)	total octene content (mol %)	hard block content (wt %)	I_2 (g/10 min)	M_w (kg/mol)	M_w/M_n
EO18.9	SS	48.3	18.9	0	1.2	129	2.1
$(EO0.5)_{18}$-*b*-$(EO18.9)_{82}$	H18	39.8	14.2	18	1.7	112	2.0
$(EO0.5)_{27}$-*b*-$(EO18.9)_{73}$	H27	35.6	12.2	27	1.4	124	2.1
$(EO0.5)_{40}$-*b*-$(EO18.9)_{60}$	H40	29.6	9.5	40	1.0	110	2.0
$(EO0.5)_{57}$-*b*-$(EO18.9)_{43}$	H57	22.0	6.6	57	1.0	108	1.9
$(EO0.5)_{67}$-*b*-$(EO18.9)_{33}$	H67	17.4	5.0	67	1.1	100	1.9
$(EO0.5)_{82}$-*b*-$(EO18.9)_{18}$	H82	10.1	2.7	82	1.0	102	1.9
EO0.5	HS	2.0	0.5	100	4.0	77	1.8

Table 2. Physical Properties of Blocky Ethylene−Octene Copolymers

polymer	density (g/cm^3)	$X_{c,r}$[a] (wt %)	T_m (°C)	ΔH_m (J g^{-1})	$X_{c,\Delta H}$[b] (wt %)	T_c (°C)	$X_{c,WAXD}$[c] (wt %)	T_g(DMTA)[d] (°C)	T_a(DMTA)[d] (°C)
SS	0.8582							−44	
H18	0.8649	8	114	19	7	74	6	−43	
H27	0.8795	19	118	49	17	94	19	−42	91
H40	0.8929	29	119	79	27	98	30	−40	91
H57	0.9022	36	121	89	31	100	35	−34	95
H67	0.9097	41	122	115	40	101	41	−31	97
H82	0.9202	49	124	137	47	104	50	−19	98
HS	0.9349	59	126	170	59	109	57		98

[a] Crystallinity from density. [b] Crystallinity from heat of melting. [c] Crystallinity from WAXD. [d] From tan δ, T_β is taken as T_g.

the anionic block copolymers, to emphasize the important differences resulting from the blocky architecture.

Materials and Methods

The blocky ethylene−octene (EO) copolymers synthesized by the chain-shuttling method,[30] were supplied as pellets by The Dow Chemical Company together with information on octene content, molecular weight, and molecular weight distribution as given in Table 1. Results from the statistical analysis of the chain-shuttling phenomenon were also provided by Dow. Homogeneous EO copolymers with essentially the same composition as the hard block (0.5 mol % octene) and as the soft block (18.9 mol % octene) were used as controls and are designated as HS and SS.

The weight percent hard block w_{HB} in the blocky copolymers was calculated from the weight percent total octene w_o as

$$w_{HB}(\%) = \frac{48.3 - w_o(\%)}{0.463} \quad (1)$$

taking the octene content of hard and soft blocks as 2.0 wt % and 48.3 wt %, respectively. The blocky copolymers are designated as $(EO0.5)_x$-*b*-$(EO18.9)_{100-x}$ where EO0.5 is the hard block, EO18.9 is the soft block, and *x* is the hard block content as weight percent. For convenience, a shorter sample code, H*x*, is used hereafter. The local comonomer distribution within the hard and soft blocks was statistical and homogeneous.

The product of the chain-shuttling process is a multiblock copolymer with a distribution of block lengths and a distribution in the number of blocks per chain. A statistical analysis of the chain-shuttling phenomenon revealed the copolymers to have a most probable distribution of block lengths and number of blocks per chain. Preliminary model calculations of the polymers used in this study predicted that the bulk of the polymer had between 2 and 10 blocks per chain. The molecular weight of the average hard block of an H82 chain with the weight-average molecular weight (Table 1) and 6 blocks (3 hard blocks) would be 28 kg/mol or ∼1900 C atoms in the backbone. The corresponding values would be 22 kg/mol or ∼1500 C atoms for H67; 21 kg/mol or ∼1400 C atoms for H57; 15 kg/mol or ∼1000 C atoms for H40; 11 kg/mol or ∼800 C atoms for H27; and 7 kg/mol or ∼500 C atoms for H18.

Films 0.5 mm thick were compression molded from the pellets. The pellets were sandwiched between Mylar sheets and preheated at 190 °C for 5 min under minimal pressure, cycled from 0 to 10 MPa pressure for 1 min to remove air bubbles, held at 10 MPa for 4 min and cooled to ambient temperature at approximately 15 °C min^{-1} in the press. The compression molded films were subsequently stored at ambient temperature for 7−12 days before measuring the physical and mechanical properties.

Density was measured according to ASTM D1505−85 using small pieces cut from the compression molded films. A 2-propanol−water gradient column with a density range of 0.8−1.0 g cm^{-3} was used. The reported density is the average of at least three specimens and has an error of less than 0.0005 g cm^{-3}.

Specimens weighing 5−10 mg were cut from compression-molded films for thermal analysis. Thermograms were obtained on a Perkin-Elmer Series 7 differential scanning calorimeter (DSC). Scans were taken between −50 °C to 190 °C with a heating/cooling rate of 10 °C min^{-1}.

Wide-angle X-ray diffractograms (WAXD) were obtained at ambient temperature using Ni-filtered Cu Kα radiation on a Rigaku RING2200 Ultima diffractometer in the reflection mode with a scanning increment of 0.05°.

Specimens for optical microscopy (OM) were made by sandwiching a pellet between two glass slides, heating at 190 °C for 5 min under minimal pressure, and slowly cooling at 3 °C min^{-1} on a Mettler hot stage. After 1 day at ambient temperature, polarized optical microscopy was performed on the specimens with an Olympus BH-2 microscope. A λ/4-plate was used in birefringence measurements.

Free surfaces for atomic force microscopy (AFM) were prepared by melting the polymer on a glass slide at 190 °C for 5 min and cooling slowly at a rate of 3 °C min^{-1} under nitrogen in a Rheometrics DSC. The thickness of the polymer film was at least equal to the spherulite diameter. After aging 1 day at ambient temperature, the free surface was imaged in air with a commercial scanning probe microscope Nanoscope IIIa from Digital Instruments operating in the tapping mode. Images were collected at ambient conditions. In most cases, intermediate tapping force was used, however hard tapping was required for imaging blocky copolymers with low crystallinity, H27 and H18. The ratio of the set point amplitude (A_{sp}) to the free oscillation amplitude (A_o) for each AFM image is given in the figure caption. Height and phase images were recorded simultaneously. The spherulitic structure was more apparent in height images and the lamellar morphology was better revealed by the modulus difference in phase images.

Dynamic mechanical thermal analysis (DMTA) was carried out with a Polymer Laboratories dynamic mechanical thermal analyzer.

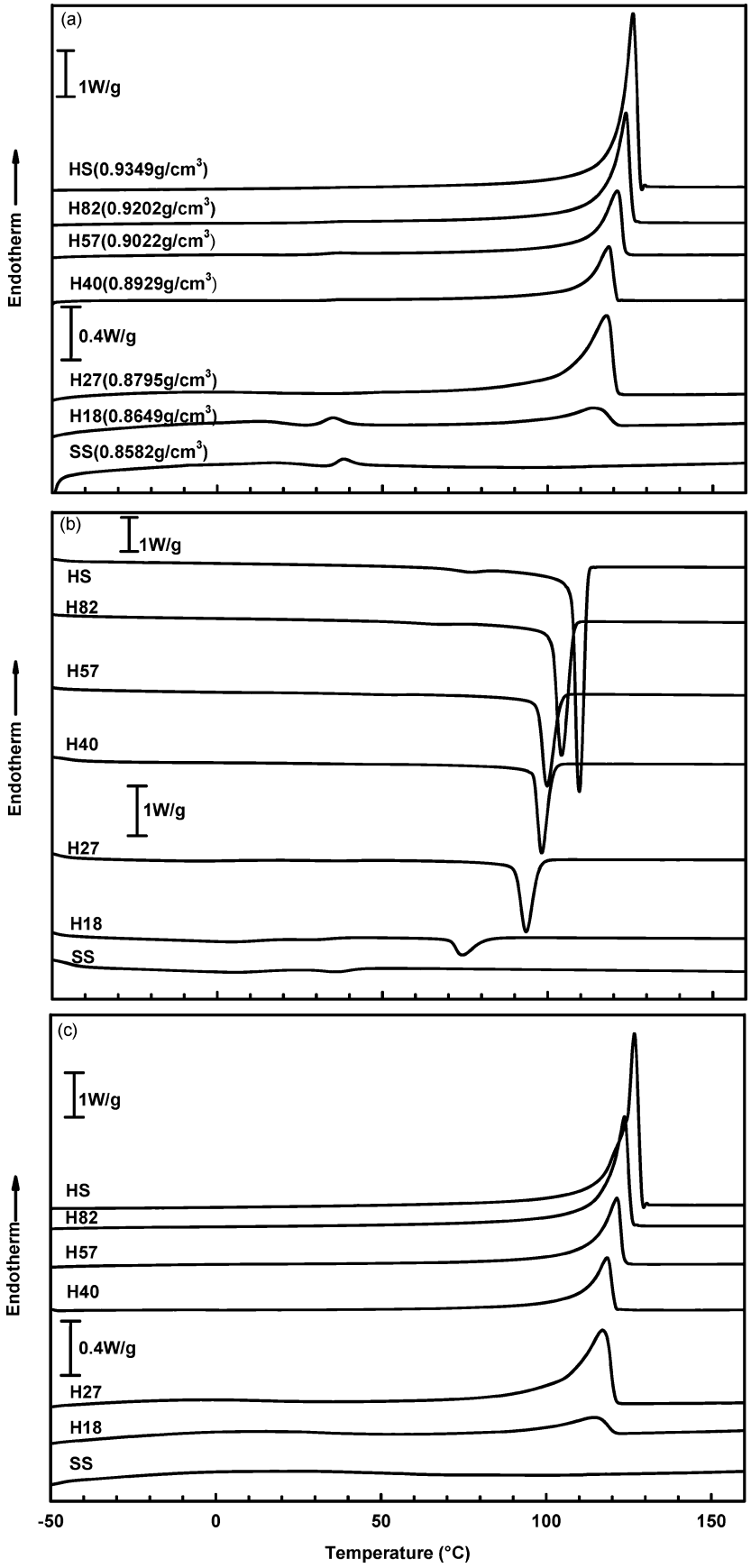

Figure 1. Thermal behavior of blocky EO copolymers: (a) first heating thermograms; (b) cooling thermograms; (c) second heating thermograms. Specimens were aged 7−12 days after compression molding. The heating/cooling rate was 10 °C min^{-1}.

A rectangular specimen with dimensions of 17 mm by 7 mm was cut from the compression molded film and tested in dynamic tension at less than 0.2% strain at 1 Hz from −80 to 10 °C below the melting temperature.

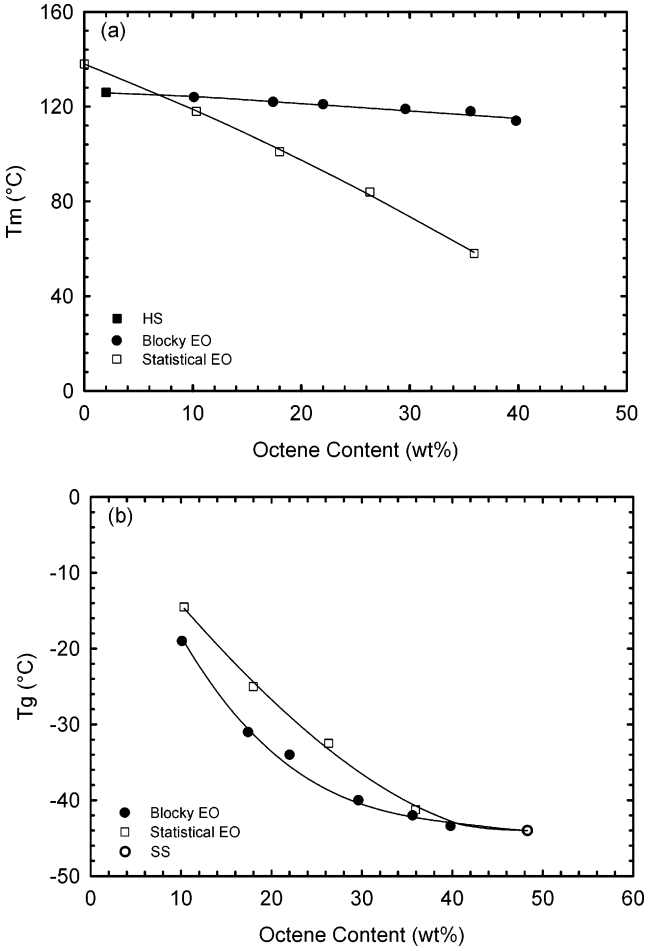

Figure 2. Effect of comonomer content on (a) melting temperature and (b) glass transition temperature: (●) blocky EO copolymers; (■) hard block; (○) soft block; (□) statistical EO copolymers. Data for statistical EO copolymers are from Bensason et al.[2] Glass transition temperature is taken as the peak temperature of the β-relaxation in the tan δ curve. The solid lines are to guide the eyes.

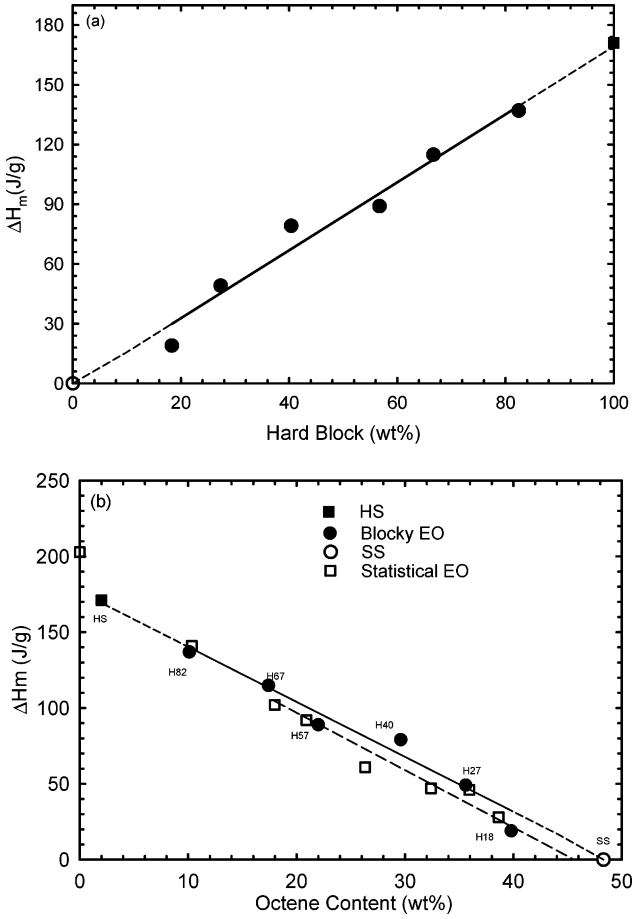

Figure 3. ΔH_m as a function of (a) hard block content and (b) comonomer content. For blocky copolymers, the solid lines are the linear least-square fits and the dashed lines give the linear extrapolations. For statistical copolymers, the dashed line is the linear least-square fit through the data. Key: (●) blocky EO copolymers; (■) hard block; (○) soft block; (□) statistical EO copolymers. Data for statistical EO copolymers are from Bensason et al.[2]

The stress−strain behavior in uniaxial tension was measured with ASTM D1708 microtensile specimens cut from the compression molded films. The separation of the grips was 22.3 mm including the fillet section; the specimen width was 4.8 mm. Specimens were stretched in an MTS Alliance RT30 at a strain rate of 500% min^{-1} at ambient temperature. Engineering stress and strain were defined conventionally. A pattern was coated on some of the specimens by depositing a gold layer over a square grid. These specimens were photographed during deformation to obtain the specimen profile. For recovery measurements, specimens were stretched to 300% engineering strain, the lower grip was released and the recovered length was measured after 10 min.

Results and Discussion

Thermal Behavior. The first heating, cooling, and the subsequent heating thermograms for blocky EO copolymers are shown in Figure 1. All of the blocky copolymers showed sharp melting and crystallization peaks. The peak temperatures shifted only slightly as the amount of crystallizable hard block decreased. The primary effect of composition was a decrease in the transition enthalpies. The results for the peak melting temperature (T_m), the heat of melting (ΔH_m), and the crystallization temperature (T_c) are summarized in Table 2. The homogeneous copolymer HS, which had the same comonomer content as the hard block, showed a peak melting temperature at 126 °C. In H82, the hard block melting peak appeared at a slightly lower temperature of 124 °C. With increasing soft block content the melting peak temperature of the hard block decreased only slightly, whereas the heat of melting decreased proportionally to the hard block content. Small changes in T_c paralleled the decrease in T_m, with the result that the undercooling (T_m −

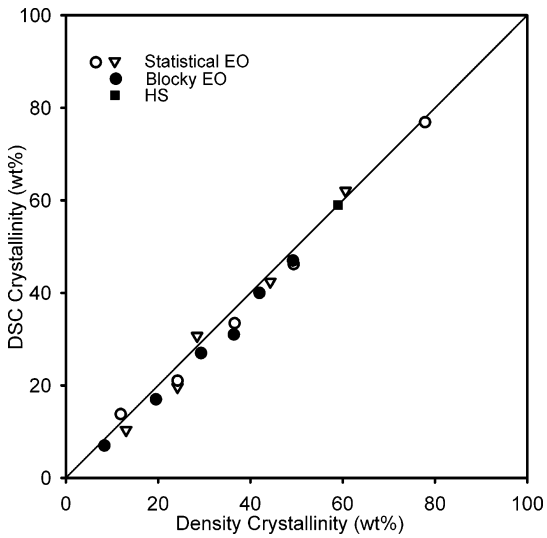

Figure 4. Comparison of crystallinity from density and crystallinity from DSC heat of melting. Key: (●) blocky EO copolymers; (■) hard block; (○, ▽) statistical EO copolymers. Data for statistical EO copolymers are from Bensason et al.[2]

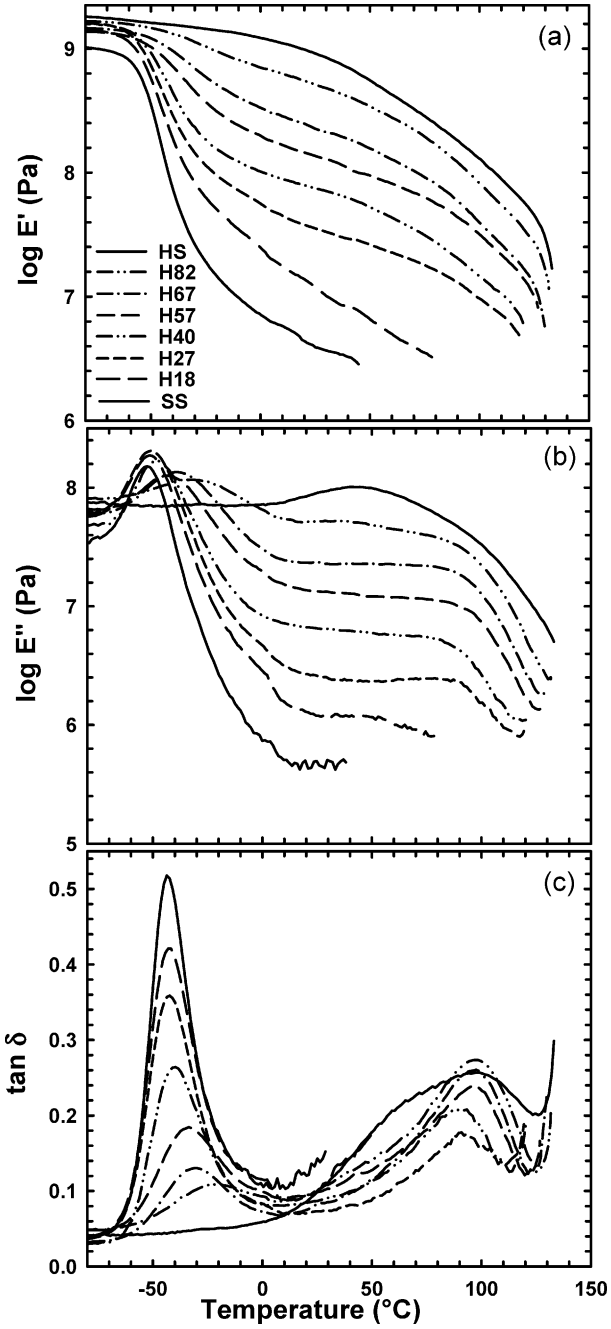

Figure 5. Dynamic mechanical relaxation behavior of blocky EO copolymers: (a) log E'; (b) log E''; (c) tan δ.

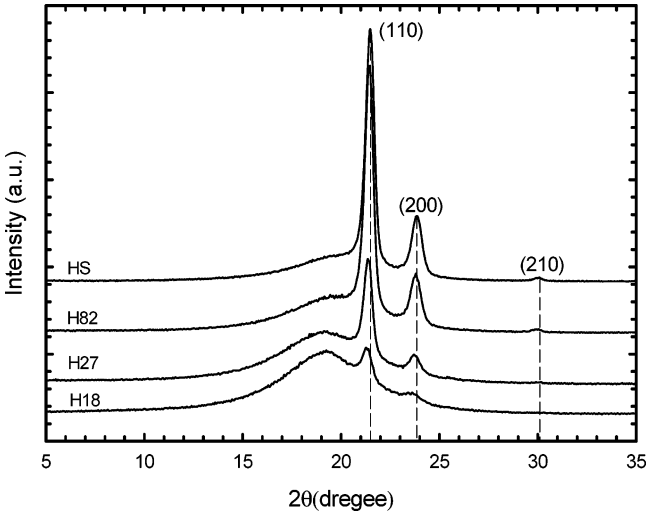

Figure 6. Wide-angle X-ray diffractograms of blocky EO copolymers.

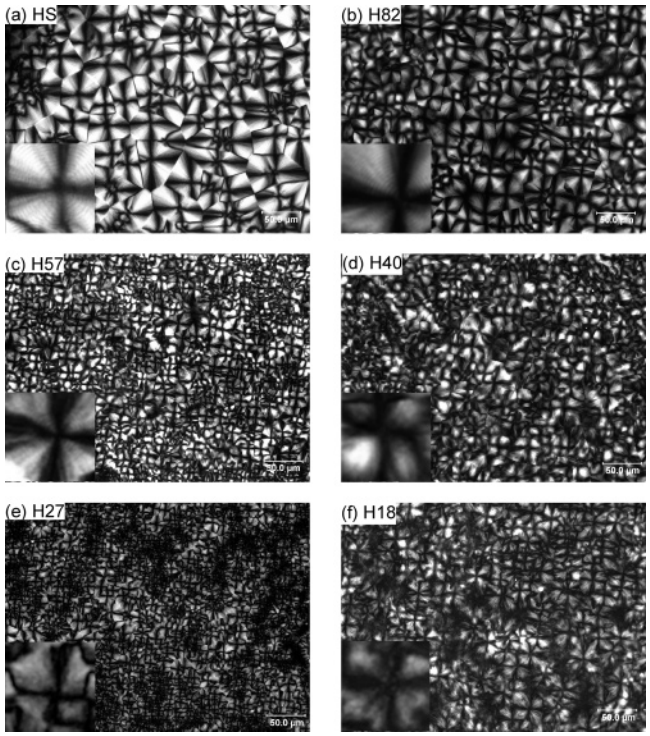

Figure 7. Polarized optical micrographs of blocky EO copolymers: (a) HS; (b) H82; (c) H57; (d) H40; (e) H27; (f) H18. The inserts are 20 μm by 20 μm areas.

T_c) was about 20 °C for HS and for all the blocky copolymers except H18.

The sharp melting peak and high melting temperature were substantially different from the thermal behavior of homogeneous statistical EO copolymers, where the melting endotherm broadened considerably and shifted rapidly to lower temperature with increasing comonomer content.[2] The sizable difference was seen by comparing the peak melting temperature of blocky and statistical EO copolymers in Figure 2a. The broad crystal size distribution and defect distribution in statistical EO copolymers resulted from the statistical distribution of crystallizable chain lengths,[3] whereas large, less defective crystals formed from the long ethylene runs in the hard blocks of the blocky copolymers.

The small low-temperature melting peak at about 37 °C in the first heating thermogram of H18 was identified with ambient temperature aging of the soft blocks.[3] It disappeared from the second heating thermogram (Figure 1c). A similar aging peak in the thermogram of the homogeneous copolymer SS, which had the same comonomer content (18.9 mol %) as the soft block, confirmed this interpretation. A previous study indicated that 15−17 mol % octene was required to achieve a completely amorphous statistical EO copolymer.[2]

The value of ΔH_m taken from the first heating thermogram decreased linearly with decreasing hard block content, Figure 3a. The linear relationship between ΔH_m and hard block content w_{HS} can be described as

$$\Delta H_m(\mathrm{J\ g^{-1}}) = 1.69 w_{HS} \qquad (2)$$

The linear relationship extrapolated to $\Delta H_m = 0$ for 100% soft block, which was consistent with the negligible crystallinity of SS. The linear relationship further indicated that the hard

block crystallinity was constant across the composition range from H82 to H27, and equal to 58 wt % taking $\Delta H_m°$ of 290 J g^{-1} for the polyethylene crystal.[31] The exception was H18, which exhibited somewhat lower crystallinity than anticipated from the linear relationship. It was noted that this polymer also crystallized with a higher undercooling than the other blocky copolymers.

The dependence of ΔH_m on total comonomer content for blocky copolymers is compared with data from the literature for statistical copolymers in Figure 3b. Extrapolation of the linear relationship for statistical copolymers to $\Delta H_m = 0$ identified 17.3 mol % (45.6 wt %) as the lowest octene content for an amorphous copolymer. The octene content of the soft segment of 18.9 mol % (48.2 wt %) was slightly higher than this. This result, combined with the linear dependence of ΔH_m on hard block content, led to a slightly higher crystallinity for a blocky copolymer compared to a statistical copolymer of the same total octene content.

The weight fraction crystallinity ($X_{c,\Delta H}$) based on the total copolymer (hard block plus soft block) is calculated as

$$X_{c,\Delta H}(\text{wt \%}) = \frac{\Delta H_m}{\Delta H_m{}^o} \times 100 \tag{3}$$

The results are compared with the weight fraction crystallinity from density ($X_{c,\rho}$) assuming a two-phase model with constant amorphous phase and crystalline phase densities

$$X_{c,\rho}(\text{wt \%}) = \frac{\rho_c}{\rho}\left(\frac{\rho - \rho_a}{\rho_c - \rho_a}\right) \times 100 \tag{4}$$

where ρ, ρ_a, and ρ_c are the bulk density, amorphous phase density and crystalline phase density, respectively. Using the generally accepted values of ρ_a and ρ_c for polyethylene of 0.855 and 1.000 g cm^{-3}, respectively,[32] crystallinity from density agreed quite well with crystallinity from DSC heat of melting, Figure 4. A good one-to-one correlation of these two crystallinity determinations was also found for statistical EO copolymers and results from the literature are included in Figure 4.[2] Both statistical and blocky EO copolymers can be described satisfactorily using a simple two-phase model of crystalline phase and amorphous phase. However, it is noted that the amorphous phase of the blocky copolymers has two contributions, both with essentially the same density. One contribution is from the amorphous soft block and the other is from the noncrystalline regions of the hard block.

Dynamic Mechanical Relaxations. The dynamic mechanical relaxation behavior of the blocky copolymers, HS and SS is shown as storage modulus (E'), loss modulus (E'') and loss tangent (tan δ) in Figure 5. Two primary relaxations were observed in the temperature range examined. They were conventionally identified as the crystalline α-relaxation and the lower temperature amorphous β-relaxation. The α-relaxation at about 98 °C in tan δ was the most intense relaxation of HS. A decrease in α-relaxation intensity paralleled the decrease in hard block content. However, T_α decreased only slightly from 98 °C for H82 to 91 °C for H27, Table 2. The α-relaxation was not recorded in H18 due to softening and flow of this composition. In contrast, decreasing crystallinity of statistical EO copolymers was characterized by a substantial decrease in T_α until the α-relaxation overlapped with the β-relaxation.[2]

The β-relaxation is usually identified as the glass transition of ethylene copolymers.[33−35] Thus, the primary relaxation of the copolymer SS was the very intense β-relaxation peak at −44 °C in tan δ which was accompanied by a drop in storage modulus of more than 2 orders of magnitude. The blocky copolymers with high soft block content, H27 and H18, also exhibited an intense β-relaxation at the same temperature as the peak in SS. This suggested that the soft block mobility was not significantly affected by the hard block crystallization. With increasing hard block content, the β-relaxation decreased in intensity and moved to slightly higher temperature. In these compositions, it appeared that the soft block mobility was reduced somewhat due to restrictions imposed by the crystalline phase.[36] However, T_β increased to only −19 °C in H82. The octene content had a much larger effect on the T_β of statistical copolymers, as shown by the comparison in Figure 2b. The effect was especially noticeable in copolymers with higher crystallinity, where the blocky copolymer could have T_β 10 °C lower than the statistical copolymer of the same octene content.

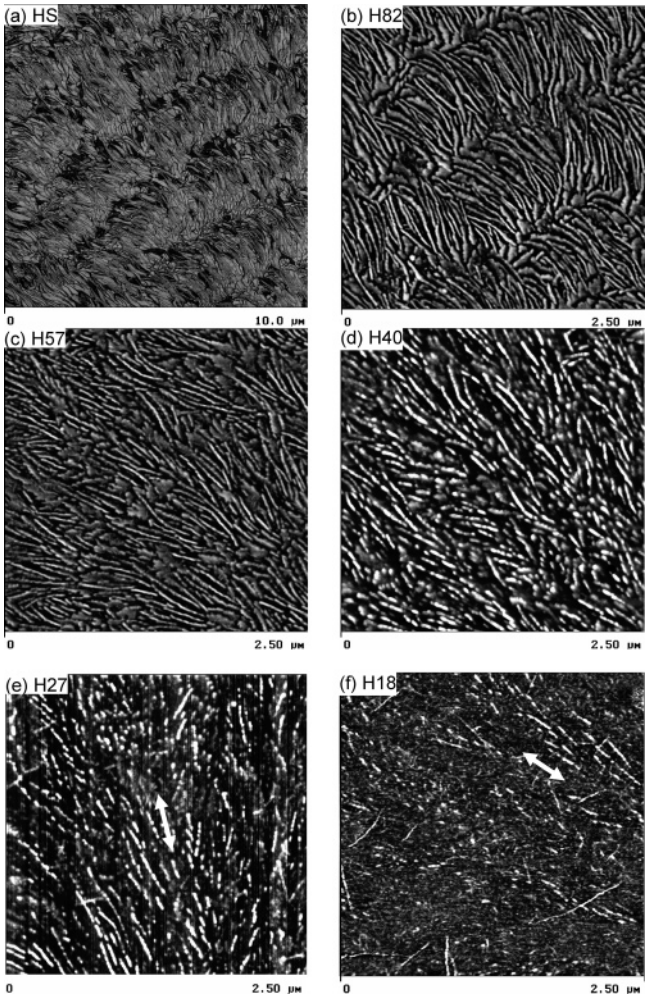

Figure 8. Free surface AFM phase images of blocky EO copolymers: (a) HS ($A_{sp}/A_o = 0.80$); (b) H82 ($A_{sp}/A_o = 0.70$); (c) H57 ($A_{sp}/A_o = 0.60$); (d) H40 ($A_{sp}/A_o = 0.70$); (e) H27 ($A_{sp}/A_o = 0.48$); (f) H18 ($A_{sp}/A_o = 0.44$). Arrows indicate the radial direction. Note the different scale in the image of HS.

The peak β-relaxation temperature in the tan δ curve is given as T_g(DMTA) in Table 2. It has been suggested that the peak temperature in E'' should be taken as T_g, rather than the commonly used definition from the tan δ curve.[37] The peak temperature in the E'' curve was about 10 °C lower than that in the tan δ curve.

Crystal Structure. The WAXD patterns are shown in Figure 6. In copolymer HS, the peaks at 2θ of 21.50, 23.90, and 30.05° were assigned to the (110), (200), and (210) crystallographic

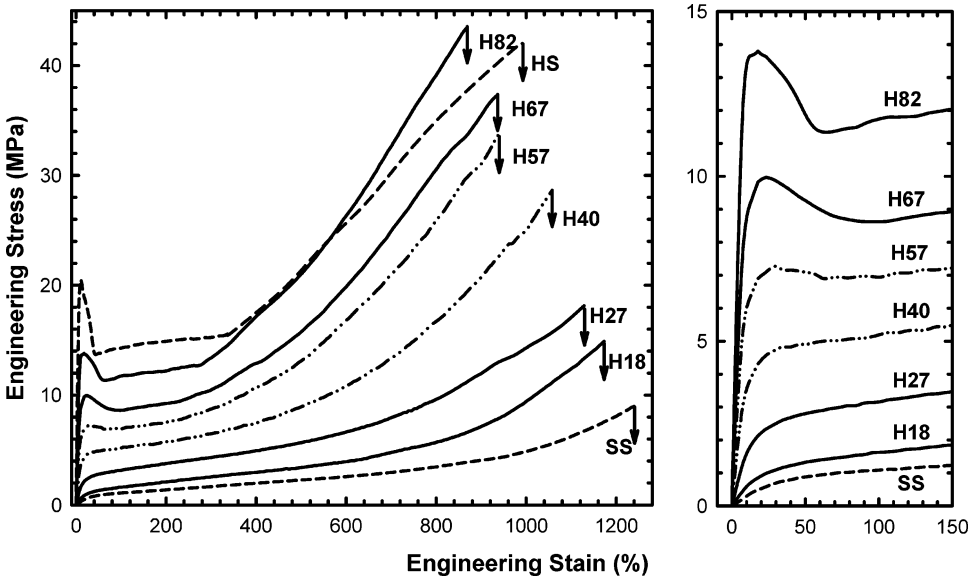

Figure 9. Engineering stress−strain curves of blocky EO copolymers and copolymers HS and SS at 23 °C. The strain rate was 500%/min.

Table 3. Tensile Properties of Blocky Ethylene−Octene Copolymers

polymer	density (g/cm^3)	$X_{c,\Delta H}$ (wt %)	5% secant modulus (MPa)	yield stress (MPa)	fracture stress (MPa)	fracture strain (%)	recovery[a] (%)
SS	0.8582		3.0	0.80	8.9	1239	95
H18	0.8649	7	5.9 ± 0.2	1.2 ± 0.1	14 ± 2	1234 ± 54	94
H27	0.8795	17	18 ± 1	2.5 ± 0.2	17 ± 3	1096 ± 66	85
H40	0.8929	27	43 ± 2	5.1 ± 0.1	26 ± 3	1042 ± 66	68
H57	0.9022	31	72 ± 1	7.3 ± 0.2	32 ± 3	925 ± 36	62
H67	0.9097	40	98 ± 1	10.4 ± 0.5	35 ± 1	896 ± 40	47
H82	0.9202	47	166 ± 2	13.7 ± 0.8	42 ± 3	831 ± 37	28
HS	0.9349	59	275 ± 3	19.9 ± 0.4	43 ± 2	997 ± 53	14

[a] Strain recovery from 300% strain

planes of the orthorhombic unit cell of polyethylene. With increasing soft block content, the two strongest reflections of the orthorhombic unit cell persisted, but the intensity decreased, whereas the intensity of the broad amorphous halo increased.[38] The small shift of the crystalline peaks to lower scattering angle with increasing soft block content suggested that the orthorhombic unit cell was slightly dilated due to chain branching.[38] However, the distortion was much less than reported in statistical EO copolymers. The diffraction peaks of the orthorhombic unit cell of a statistical copolymer with crystallinity intermediate between H18 and H27 were much more diffuse and shifted to much lower angles.[39] It has been suggested that the crystal defects in the statistical EO copolymers are enough to produce some amount of hexagonal form.[40,41] The hexagonal form was not observed in any of the blocky copolymers.

By resolving the multiple-peak pattern into the individual crystalline peaks and an amorphous halo,[42] the weight percent crystallinity was estimated from WAXD using

$$X_{c,WAXD}(\text{wt \%}) = \frac{A_c}{A_c + A_a} \times 100 \qquad (5)$$

where A_c is the total area under the crystalline peaks and A_a is the area under the amorphous halo. The results given in Table 2 correlated well with the other two crystallinity determinations, confirming the good phase separation in the solid state.

Solid-State Morphology. Polarized light micrographs in Figure 7 illustrate the effect of soft block content on the spherulitic morphology. Copolymer HS showed space-filling spherulites about 36−44 μm in diameter. Large, space-filling spherulites were also observed in all the blocky copolymers, even H18 which had only 7 wt % crystallinity. The spherulite diameter decreased somewhat from ∼30 μm in H82 to ∼18 μm in H18. However, the primary effect of decreasing hard block content was to reduce the intensity of the birefringence pattern. All the spherulites exhibited negative birefringence, which is typical of polyethylene spherulites. The negative birefringence indicated that a significant fraction of the lamellae were oriented radially with the chain direction tangential. The banding pattern became progressively weaker from HS to H57, as seen in the inset in Figure 7a−c, and disappeared from H40 onward.

The corresponding high-resolution AFM phase images of the free surfaces in Figure 8 revealed lamellar structures in all the blocky copolymers. Banding was observed in HS, H82, and H57, which was consistent with the optical microscopy. The higher resolution of the AFM allowed measurements of the band spacing. In HS regular twisting of lamellar ribbons with a spacing of about 2.5 μm was clearly seen. The band spacing decreased to about 0.9 μm for H82. The banding was irregular in H57 and was lost from H40 onward.

Predominantly radial orientation of the lamellae confirmed the interpretation of the birefringence pattern in the optical microscope. The primary effect of increasing soft block content was to decrease the packing density of the lamellae due to accommodation of a larger fraction of amorphous material in the interlamellar regions. In addition, the lamellae of H27 and H18 were more fragmented and acquired a segmented appearance much like a string of beads. However, even in H18, lamellar fragments as long as 200 nm were seen.

The spherulitic and lamellar morphologies were consistent with crystallization of hard blocks from a homogeneous melt.

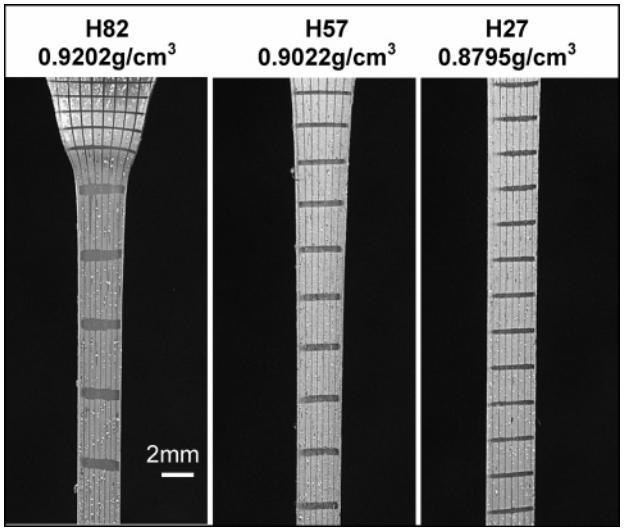

Figure 10. Photographs of tensile specimens at 150% engineering strain.

Crystallization from a strongly microphase-separated melt would have resulted in a domain morphology of spheres, rods or lamellae, such as observed in sPP-*b*-EPR and sPP-*b*-PE.[18c] Rather, it appeared that crystallization of the hard blocks forced segregation of the noncrystallizable soft blocks into the interlamellar regions. Crystallization of blocky copolymers as spherulites, rather than as domains, was observed previously in block copolymers with well-defined block lengths. Spherulites of hydrogenated (polybutadiene-*b*-polyisoprene) (hPB-*b*-hPI) were attributed to crystallization from a single-phase melt.[20,26] Furthermore, spherulites of hPB-*b*-hPI with only 12 wt % crystallizable block were reported.

Although spherulitic organization of lamellar crystals is generally associated with long chain polymers, it is also observed in *n*-alkanes and in crystallizable blocks that are long enough to chain fold (about 200 carbon atoms). Lamellar crystallization results from the tendency of crystallizable segments to attach progressively to a preferred growth plane. The spherulitic arrangement is thought to result from the pressure of uncrystallized segments emerging from the lamellar surfaces, which causes the dominant lamellae to diverge.[43]

Good separation of the hard block lamellar crystals from the interlamellar soft blocks was confirmed by distinct and separate β- and α-relaxations in all the blocky copolymers. The α-relaxation is usually identified with the crystalline phase of polyethylene. It is attributed to chain translation along the crystalline axis.[44] The reported decrease in the α-relaxation temperature with decreasing lamellar thickness supports this interpretation.[33] However, it has been noted that the translational component of the crystal stem motion is coupled to amorphous chain blocks at the crystal surface.[34] Thus, the mobility of crystal chain stems also depends on the degree of surface order. Indeed, the strong effect of cooling rate on the α-relaxation of a statistical EO copolymer suggests that the degree of surface order may be more important than the lamellar thickness.[2] It follows from the almost constant α-relaxation temperature of blocky copolymers that the lamellar crystals retained a high degree of surface order, with good separation of the crystalline hard blocks and the interlamellar amorphous blocks, even in the copolymers with very low hard block content.

Stress−Strain Behavior. The uniaxial stress−strain behavior of the blocky copolymers ranged from that typical of a semicrystalline thermoplastic, with localized yielding and necking, to that of an elastomer, characterized by uniform deformation and high recovery from large strain, Figure 9. The sharp yielding maximum in the stress−strain curves of H82 and H67 was in contrast to the complex double yielding that characterized homogeneous statistical copolymers of similar octene content.[45−48] The tensile properties listed in Table 3 include the secant modulus at 5% strain, the yield stress, and the ultimate stress and strain for all the blocky copolymers, as well as the values for HS and SS.

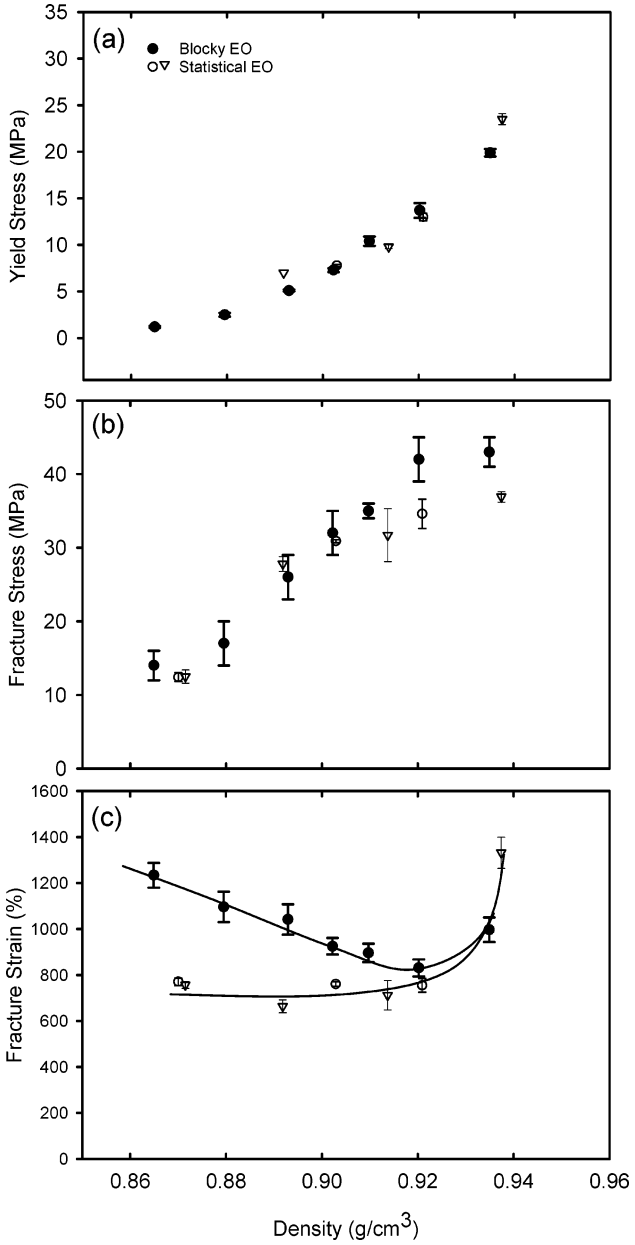

Figure 11. Comparison of mechanical properties of blocky EO and statistical EO copolymers as a function of density (i.e., crystallinity): (a) yield stress; (b) fracture stress; (c) fracture strain. Data of statistical EO copolymers are from Bensason et al.[2]

The distinctive features of yield behavior inferred from the stress−strain curves are illustrated with photographs of the specimens at 150% engineering strain, Figure 10. The blocky copolymer with highest hard block content, H82, showed behavior typical of a semicrystalline thermoplastic. Highly localized yielding produced a well-defined neck, which propagated along the gauge length in a stable manner. Cold drawing of the neck was followed by uniform strain-hardening at high strains. The H82 specimens exhibited very little recovery after fracture.

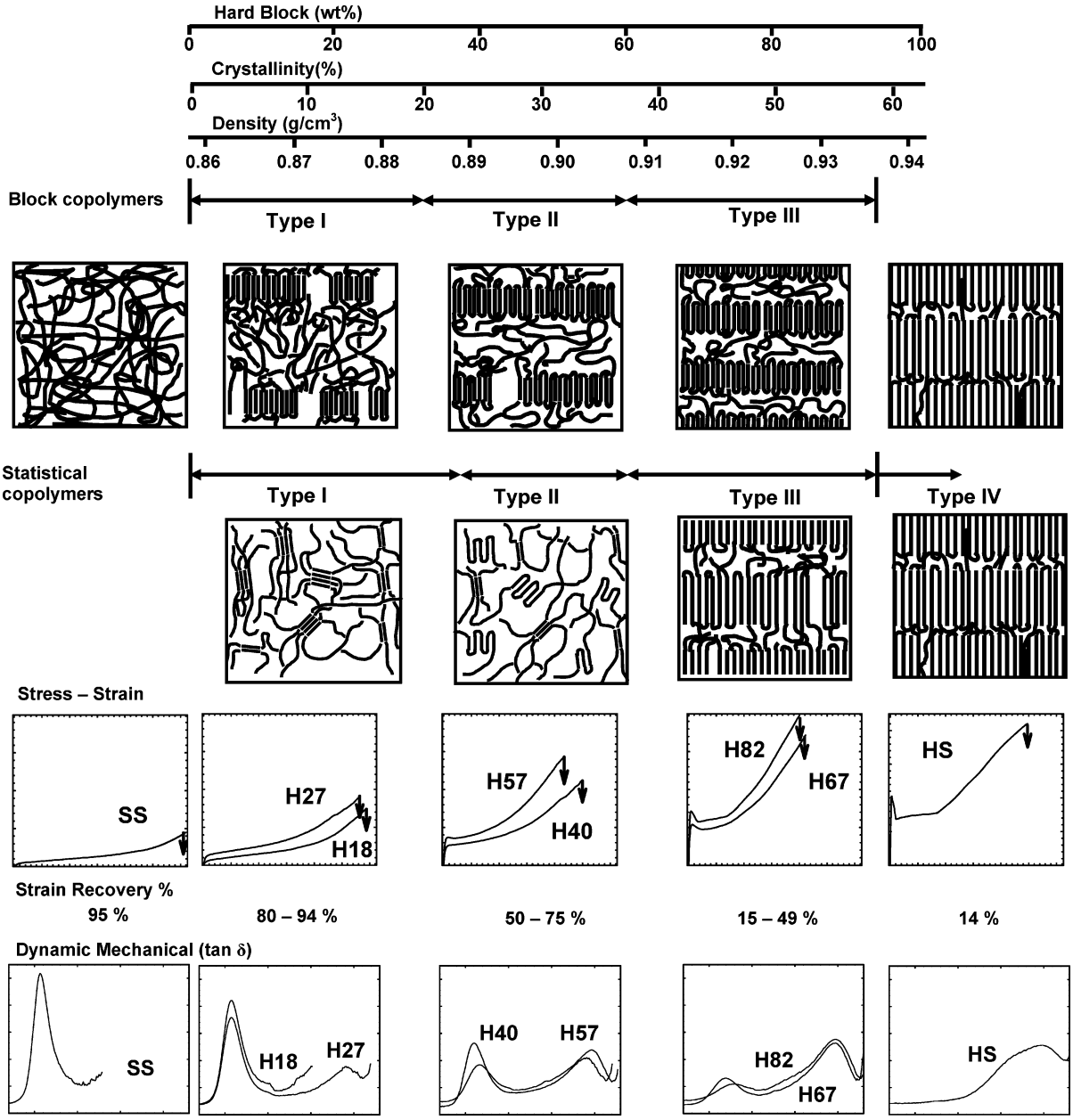

Figure 12. Classification schemes of blocky and statistical EO copolymers based on hard block content.

With increasing soft block content, the modulus decreased, the yield stress decreased, and the neck became more diffuse. The nonuniform cold drawing region of the stress−strain curve became shorter until it disappeared and only uniform strain hardening was observed. Concurrently, the slope of the strain hardening region decreased. Diffuse necking of H57 is illustrated in Figure 10 by a very gradual transition from the closer line spacing on the less deformed region at the top of the photograph to the more widely spaced markings at the bottom.

The deformation of H27 was macroscopically uniform. The spacing of the marks in Figure 10 corresponded to the macroscopic strain. The deformation showed elastomeric characteristics with a low initial modulus, a gradual increase in the slope of the stress−strain curve at higher strains and large instantaneous strain recovery after fracture. Copolymer SS with virtually no crystallinity exhibited very low strength, and only a small amount of strain-hardening before fracture. High extensibility and considerable strain recovery of SS were attributed to chain entanglements.

The yield stress, a bulk property that typically depends on total crystallinity, showed the same dependence on crystallinity, as reflected by density, for blocky and statistical copolymers, Figure 11a. Similarly, the dependence of fracture stress on crystallinity was comparable for blocky and statistical copolymers, Figure 11b. However, because of the higher melting temperature of blocky copolymers, it was anticipated that they would maintain mechanical properties to higher temperatures than the statistical copolymers. The blocky copolymers also possessed higher extensibility before fracture than the statistical copolymers, Figure 11c.

Classification of Blocky EO Copolymers. The fundamental difference in chain architecture of blocky and statistical EO copolymers has considerable impact on the crystallization behavior. The blocky architecture imparts a substantially higher crystallization temperature, a higher melting temperature, and a better organized crystalline morphology. The differences become progressively more apparent as the total comonomer content increases and the crystallizable sequences in the

statistical copolymer become increasingly shorter compared to the long crystallizable sequences that persist in the blocky copolymer.

Crystallization of the blocky copolymers as space-filling spherulites with radial lamellar organization is consistent with crystallization from a homogeneous melt. Although the hard and soft blocks differ considerably in the comonomer content, the blocks are short enough to be miscible in the melt.[28] Upon cooling, crystallization of the hard blocks forces segregation of the noncrystallizable soft blocks into the interlamellar regions. The crystallizable blocks are long enough to form well-organized lamellar crystals with the orthorhombic unit cell and high melting temperature. Good separation of hard and soft blocks is confirmed by distinct and separate β- and α-relaxations in all the blocky copolymers. This is in contrast to the statistical copolymers where decreasing length of the crystallizable sequences results in smaller and more defective crystalline structures as the comonomer content increases. Despite the fundamental differences in crystallization habit, a bulk property such as the yield stress exhibits a common dependence on crystallinity for blocky and statistical copolymres.

Like the statistical copolymers, the blocky EO copolymers present a broad range of properties, ranging from thermoplastic characteristics of H82 to elastomeric behavior of H18. Although the property changes occur gradually with the relative amounts of alternating crystallizable and amorphous blocks, it is useful to categorize the polymers based on composition, Figure 12. Correspondence in the relationship between crystallinity and comonomer content facilitates comparisons with a similar classification scheme for statistical EO copolymers,[2] which is included in the figure. Indeed, the blocks are statistical copolymers that bracket the usual range in copolymer composition, and therefore HS and SS are included at the ends of the composition range.

With very low comonomer content and density about 0.94 g cm^{-3}, HS closely resembles HDPE.[2,49] It is characterized by large negative spherulites with thick, well organized lamellae. Type III copolymers are LLDPE-like with 0.91−0.92 g cm^{-3} density and 40−50% crystallinity. Both blocky and statistical copolymers in this category crystallize as banded space-filling spherulites with closely packed radial lamellae. They deform by yielding with a sharp neck. However, the effect of the blocky architecture is evident. Because of longer crystallizable sequences, blocky type III copolymers have crystallization and melting temperatures about 10 °C higher than LLDPE. The melting temperature is about 20 °C higher than that reported for olefinic block copolymers synthesized by anionic polymerization and hydrogenation.[26−29] For the latter, some amount of 1,2-substitution in the crystallizable blocks introduces branches, which are responsible for the lower melting temperature.

Plastomer type II blocky copolymers, exemplified by H57 and H40, have density of 0.89−0.90 g cm^{-3} and crystallinity of 25−35%. They exhibit slightly smaller spherulites than type III. The presence of discontinuous lamellae differentiates type II from type III. As a result of lamellar discontinuities, the regular banding pattern is not observed. In contrast, type II statistical EO copolymers crystallize as a mixture of short lamellar crystals and fringed micellar crystals. Type II statistical copolymers can form spherulites if they are slowly cooled from the melt, however the radial organization of the lamellae is not as well-developed as in the spherulites of type II blocky copolymers.[2]

With density of 0.87−0.88 g cm^{-3} and crystallinity less than 20%, elastomeric H27 and H18 are classified as type I. They are characterized by space-filling spherulites. The short, discontinuous lamellae have predominately radial orientation. This is in sharp contrast to statistical copolymers of similar crystallinity. Type I statistical copolymers exhibit a mottled birefringence pattern and granular morphology of small fringed micellar crystals.[2] In both blocky and statistical type I copolymers, crystals act as the physical cross-links that impart large recovery from high strain. However, it can be anticipated that the lamellar crystals of the blocky copolymers will be stronger and more temperature stable than the fringed micellar crystals of the statistical copolymers.

Conclusions

Characterization of the solid-state structure and properties of the new olefinic blocky copolymers reveals that they conform to the concept of a thermoplastic elastomer in which crystallizable blocks with lower octene content serve as physical cross-links to connect amorphous rubbery blocks with higher octene content. The properties of the blocky copolymers range from thermoplastic to elastomeric depending on the relative amounts of hard and soft blocks. Compared to statistical ethylene−octene copolymers, the blocky architecture imparts a substantially higher crystallization temperature, a higher melting temperature while maintaining a lower glass transition temperature, and a better organized crystalline morphology. The hard blocks crystallize as space-filling spherulites even when the fraction of crystallizable hard blocks is very low. Good separation of hard and soft blocks is confirmed by distinct and separate β- and α-relaxations in all the blocky copolymers. The difference between blocky and statistical copolymers is most apparent in the elastomeric compositions with high comonomer content. Although crystals act as the physical cross-links that impart high recovery to both blocky and statistical copolymers, it is anticipated that the lamellar crystals of the blocky copolymers will be stronger and more temperature stable than the fringed micellar crystals of the statistical copolymers.

Acknowledgment. The authors thank The Dow Chemical Company for their financial and technical support.

References and Notes

(1) Sehanobish, K.; Patel, R. M.; Croft, B. A.; Chum, S. P.; Kao, C. I. *J. Appl. Polym. Sci.* **1994**, *51*, 887−894.
(2) Bensason, S.; Minick, J.; Moet, A.; Chum, S.; Hiltner, A.; Baer, E. *J. Polym. Sci., Part B: Polym. Phys.* **1996**, *34*, 1301−1315.
(3) Minick, J., Moet, A., Hiltner, A., Baer, E., Chum, S. P. *J. Appl. Polym. Sci.* **1995**, *58*, 1371−1384.
(4) Bensason, S.; Stepanov, E. V.; Chum, S.; Hiltner, A.; Baer, E. *Macromolecules* **1997**, *30*, 2436−2444.
(5) *Thermoplastic Elastomers*, 3rd ed.; Holden, G., Kricheldorf, H. R., Quirk, R. P., Eds.; Hanser Publishers: Munich, Germany, 2004.
(6) Kontos, E. G.; Easterbrook, E. K.; Gilbert, R. D. *J. Polym. Sci*. **1962**, *61*, 69−82.
(7) (a) Busico, V.; Corradini, P.; Fontana, P.; Savino, V. *Macromol. Chem. Rapid Commun.* **1984**, *5*, 737−743. (b) Busico, V.; Corradini, P.; Fontana, P.; Savino, V. *Macromol. Chem. Rapid Commun.* **1985**, *6*, 743−747.
(8) Lock, G. A. Thermoplastic Elastomers Based on Block Copolymers of Ethylene and Propylene. In *Advances in Polyolefines*; Seymour, R. B., Cheng, T., Eds.; Plenum Press: New York, 1985.
(9) Wang, L.; Huang, B. *J. Polym. Sci., Polym. Phys. Ed.* **1991**, *29*, 1447−1456.
(10) (a) Doi, Y.; Ueki, S.; Keii, T. *Macromolecules* **1979**, *12*, 814−819. (b) Doi, Y.; Ueki, S.; Keii, T. *Macromolecules* **1979**, *12*, 1012−1013.
(11) Doi, Y.; Ueki, S. *Macromol. Chem. Rapid Commun.* **1982**, *3*, 225−229.
(12) Doi, Y.; Keii, T. *Adv. Polym. Sci.* **1986**, *73-4*, 201−248.
(13) Coates, G. W.; Waymouth, R. M. *Science* **1995**, *267*, 217−219.

(14) Chien, J. C. W.; Iwamoto, Y.; Rausch, M. D.; Wedler, W.; Winter, H. H. *Macromolecules* **1997**, *30*, 3447−3458.
(15) Lieber, S.; Brintzinger, H.-H. *Macromolecules* **2000**, *33*, 9192−9199.
(16) (a) Zhang, Y.; Keaton, R. J.; Sita, L. R. *J. Am. Chem. Soc.* **2003**, *125*, 9062−9069. (b) Harney, M. B.; Zhang, Y. H.; Sita, L. R. *Angew. Chem. Int. Ed.* **2006**, *45*, 2400−2404.
(17) Cherian, A. E.; Rose, J. M.; Lobkovsky, E. B.; Coates, G. W. *J. Am. Chem. Soc.* **2003**, *127*, 13770−13771.
(18) (a) Tian, J.; Hustad, P. D.; Coates, G. W. *J. Am. Chem. Soc.* **2001**, *123*, 5134−5135. (b) Mason, A. F.; Coates, G. W. *J. Am. Chem. Soc.* **2004**, *126*, 16326−16327. (c) Ruokolainen, J.; Mezzenga, R.; Fredrickson, G. H.; Kramer, E. J.; Hustad, P. D. Coates, G. W. *Macromolecules* **2005**, *38*, 851−860.
(19) Furuyama, R.; Mitani, M.; Mohri, J.; Mori, R.; Tanaka, H.; Fujita, T. *Macromolecules* **2005**, *38*, 1546−1552.
(20) Rangarajan, P.; Register, R. A.; Fetters, L. J. *Macromolecules* **1993**, *26*, 4640−4645.
(21) Rangarajan, P.; Register, R. A.; Adamson, D. H.; Fetters, L. J.; Bras, W.; Naylor, S.; Ryan, A. J. *Macromolecules* **1995**, *28*, 1422−1428.
(22) Ryan, A. J.; Hamley, I. W.; Bras, W.; Bates, F. S. *Macromolecules* **1995**, *28*, 3860−3868.
(23) Ueda, M.; Sakurai, K.; Okamoto, S.; Lohse, D. J.; MacKnight, W, J.; Shinkai, S.; Sakurai, S.; Nomura, S. *Polymer* **2003**, *44*, 6995−7005.
(24) Falk, J. C.; Schlott, R. J. *Macromolecules* **1971**, *4*, 152−154.
(25) Falk, J. C.; Schlott, R. *J. Angew. Makromol.* **1972**, *21*, 17−23.
(26) Mohajer, Y.; Wilkes, G. L.; Wang, I. C.; McGrath, J. E. *Polymer* **1982**, *23*, 1523−1535.
(27) Seguela, R.; Prudhome, J. *Polymer* **1989**, *30*, 1446−1455.
(28) Koo, C. M.; Wu, L.; Lim, L. S.; Mahanthappa, M. K.; Hillmyer, M. A.; Bates, F. S. *Macromolecules* **2005**, *38*, 6090−6098.
(29) Koo, C. M.; Hillmyer, M. A.; Bates, F. S. *Macromolecules* **2006**, *39*, 667−677.
(30) Arriola, D. J.; Carnahan, E. M.; Hustad, P. D.; Kuhlman, R. L.; Wenzel, T. T. *Science* **2006**, *312*, 714−719.
(31) Wunderlich, B. *Macromolecular Physics*; Academic Press, New York, 1980; Vol. 3; p 42.
(32) Brandrup, J.; Immergut, E. H. *Polymer Handbook*, 3rd ed.; Wiley: New York, 1989; Section V/17.
(33) Popli, R.; Glotin, M.; Mandelkern, L. Benson, R. S. *J. Polym. Sci., Polym Phys Ed* **1984**, *22*, 407−448.
(34) Boyd, R. H. *Polymer* **1985**, *26*, 1123−1133.
(35) Boyer, R. F. *J. Macromol. Sci. Phys.* **1973**, *8*, 521−555.
(36) Wang, H. P.; Ansems, P.; Chum, S. P.; Hiltner, A.; Baer, E. *Macromolecules* **2006**, *39*, 1488−1495.
(37) Reiger, J. *Polymer Testing* **2001**, *20*, 199−204.
(38) Balta-Calleja, F. J.; Vonk, C. G. *X-ray scattering of synthetic polymers*; Elsevier: Amsterdam, 1989.
(39) Androsch, R. *Polymer* **1999**, *40*, 2805−2812.
(40) Androsch, R.; Blackwell, J.; Chvalun, S. N.; Wunderlich, B. *Macromolecules* **1999**, *32*, 3735−3740.
(41) de Ballasteros, O. R.; Auriemma, F.; Guerra, G.; Corradini, P. *Macromolecules* **1996**, *29*, 7141−7148.
(42) Kakudo, M.; Ullman, R. *J. Polym. Sci.* **1960**, *45*, 91−104.
(43) Bassett, D. C.; Olley, R. H.; Sutton, S. J.; Vaughan, A. S. *Polymer* **1996**, *37*, 4993−4997.
(44) Nitta, K.-H.; Tanaka, A. *Polymer* **2001**, *42*, 1219−1226.
(45) Balsamo, V.; Müller, A. J. *J. Mater. Sci. Lett.* **1993**, *12*, 1457−1459.
(46) Seguela, R.; Darras, O. *Mater. Sci.* **1994**, *29*, 5342−5352.
(47) Brooks, N. W. J.; Duckett, R. A.; Ward, I. M. *J. Polym. Sci., Part B: Polym. Phys.* **1998**, *36*, 2177−2189.
(48) Lucas, J. C.; Failla, M. D.; Smith, F. L.; Mandelkern, L.; Peacock, A. J. *Polym. Eng. Sci.* **1995**, *35*, 1117−1123.
(49) Peeters, M.; Goderis, B.; Vonk, C.; Reynaers, H.; Mathot, V. *J. Polym. Sci., Polym. Phys. Ed.* **1997**, *35*, 2689−2713.

MA061680E